# Construction and validation tests of a micro-impression creep test machine

KANG JUNG[1], HO-KYUNG KIM*[2]

[1] School of Mechanical Design Eng., Chonnam National University, Korea
[2] Dept. of Mechanical and Automotive Engineering, Seoul National University of Science and Technology
172 Kongneung-dong, Nowon-ku, Seoul, 139-722, Korea
kimhk@seoultech.ac.kr

*Abstract*— **A micro-impression creep machine was designed and developed, adopting a small punch in diameter of 150 um, displacement gage with sub-μm-scale accuracy, and a load-cell with mN-scale accuracy of in an effort to investigate the creep behavior of a small solder ball with a diameter of less than 1 mm. The creep behavior of a lead-free solder ball (Sn-3.0Ag-0.5Cu) with a diameter of 760 μm was investigated in the stress range of 8 to 60MPa and in the temperature range of 303K to 393K. We verified the appropriate performance of the developed machine by comparing the creep data from the self-made testing device to previously reported data for a magnesium alloy (AZ31). The stress exponent n for the solder ball sample was 3.7 in an intermediate stress range at 348K, indicating that glide of dislocations dragging in a solute atmosphere is the dominant creep deformation mechanism. The developed testing machine can be expected to find use in evaluating the creep strength of microelectronic solder joints.**

**Keywords:** Micro-impression creep machine, Lead-free Sn-3.0Ag-0.5Cu alloy, Solder ball, Dislocation glide mechanism

## I. INTRODUCTION

Microelectronic solder joints in service are exposed to undergo thermo-mechanical cycling at high homologous temperatures. As a consequence, the creep properties of the solders used are important for reliability predictions of microelectronic solders. The creep properties of microelectronic solders depend on the compositions of the solder alloys and their microstructures. Specifically, the microstructures of solder alloys strongly depend on the cooling rate during the soldering process. Additionally, the microstructures of solder joints in microelectronic packages may change continuously when they are in service as a result of isothermal aging-induced phase coarsening and the strain-enhanced coarsening of second-phase particles. Consequently, their creep properties are often quite different from that of the bulk alloy. Therefore, it is important to characterize the creep behavior of individual solder joints for accurate reliability predictions of microelectronic solder joints. However, conventional lap-shear and tensile creep techniques have several limitations when used to investigate actual solder joints less than 1 mm in diameter.

Recently, a localized impression creep technique was utilized in an effort to investigate its usefulness in evaluating the creep properties of materials [1-2]. The impression creep test can be defined as the penetration velocity of a cylindrical punch with a flat end into a material under a constant load and temperature. This localized creep testing technique has several advantages. Because the punch can be very small, this technique is suitable for the testing of small test pieces. Furthermore, multiple creep curves at different stress levels can be obtained on a single sample simply by changing the location of the punch or the applied load.

Several attempts have been made to investigate the creep properties of microelectronic solder joints by means of this impression creep testing technique. However, most of the impression creep experiments were performed on bulk materials using cylindrical punch of approximately 1 ~ 2 mm in diameter [3-4]. For example, Yang et al. [3] performed impression creep tests on bulk materials by modifying a rheometric solid analyzer equipped with an LVDT displacement gage using a cylindrical punch 0.61mm in diameter. Mahdudi et al. [4] performed impression creep tests using a servo-hydraulic MTS universal tensile testing machine equipped with a three-zone split furnace and a cylindrical punch 2 mm in diameter. Dutta et al. [5] used an impression punch with a diameter of 100 μm and investigated a solder ball with a diameter of 760 μm. They adopted a servo-hydraulic MTS universal tensile testing machine equipped with a three-zone split furnace.

However, the servo-hydraulic testing system is not appropriate for creep tests in which dozens of instance of creep-rate data or more are needed to characterize creep behavior as the hydraulic pump must run for a long time to produce the data, which can drive up the cost of the test. The nano-indentation system can produce creep data only in high creep-rate range, such as $10^{-1}$/s to $10^{-4}$/s due to the disadvantage of its limited operating time. In addition, indentation creep tests using a conical, pyramidal or spherical indenter do not show a steady state under a constant load.

Therefore, in this study, a micro-impression creep machine was designed and constructed in order to investigate the creep behavior of a small solder ball in low creep-rate ranges. The creep behavior of a lead-free

solder ball (Sn-3.0Ag-0.5Cu) with a diameter of 760 μm was investigated in the stress range of 8 to 60MPa and in the temperature range of 303K to 393K. The results thus obtained will provide a useful guideline for manufacturing and design engineers as they evaluate the creep strength of microelectronic solder joints.

## II. TESTING DEVICE DESIGN AND CONSTRUCTION

### 2.1 Testing device design

It is possible to conduct a creep test only in a high creep-rate range with a conventionally developed nano-indentation system equipped with an electrical furnace. However, it is very difficult to conduct a creep test continuously in a lower creep-rate range, such as $10^{-5}$ to $10^{-8}$/s, with such a system, as it will take several days or even weeks to complete the test. In this study, we chose a dead weight system for a stable loading system for a long time which can run for extended lengths of time, which is advantageous in a long-term creep test.

The design was specifically constructed to allow for the application of constant force onto a specimen. Referring to Fig. 1, the experimental equipment includes: a loading device to generate the load on the specimen; a system for measuring the load and displacement, a load train system to apply for the load onto the specimen, an X-Y-Z stage to adjust the location of the specimen, and a system base.
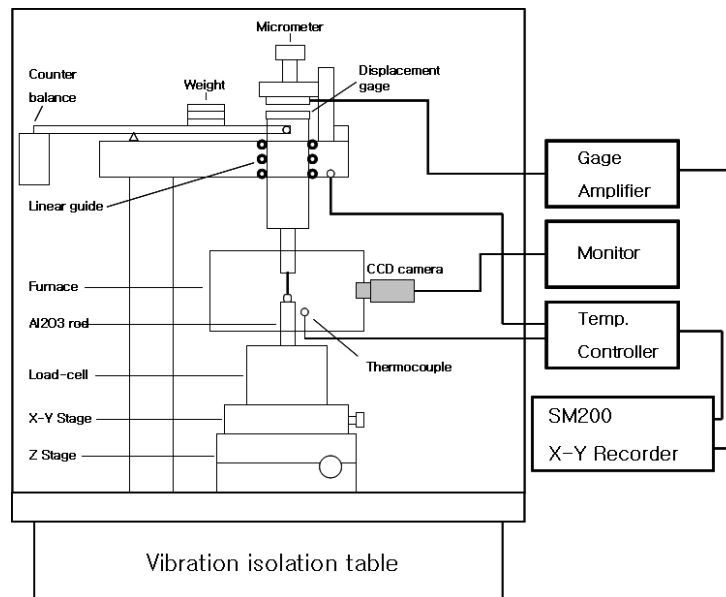


Fig. 1 Schematics of the miniature impression creep testing machine system

### 2.2 Testing device construction

The basic frame of the testing machine was manufactured using the SM45C alloy. When we apply an impression load onto a sample, there must be a weight of several kilograms in order to achieve a high impression creep rate. Therefore, a dead weight system with a variable lever ratio was chosen to apply impression force onto a creep sample. In order to impress the sample without torsion, a linear motion guide was used. The impression force was designed to be transferred from a dead weight to the sample, with alumna ($Al_2O_3$) rod with a diameter of 15 mm and a length of 40 mm and a tungsten carbide (WC + Co) punch with a diameter of 150 um.

A capacitive displacement gage (PI Co. D-050) was used to measure the creep displacement. The resolution and linearity of the sensor are 0.01nm and 0.01%, respectively. A CCD camera was used to align and adjust the gap between the plate (probe) and the other plate (target) contact of the sensor. The measuring range of the gage has to move to the proper measurement position when the punch impresses the sample to a depth that exceeds 50 um due to limited measuring range of 50 um. Therefore, a Z stage was installed to move the gage vertically. An X-Y-Z stage with a resolution of 10 um was used to adjust precisely the level and position of the punch as it impressed the sample, as shown in Fig. 2. The impression creep testing system is mounted to a vibration isolation table using an air spring.

An electrical resistance heating furnace with two band heaters was installed to heat the sample. The testing temperatures for the tests were ranged from 323 to 623K in the chamber. The temperature was controlled to within ±0.1 K. Temperature changes caused by the ambient temperature incur large amount of error in this precise creep testing system. Therefore, to eliminate displacement errors due to temperature changes, another thermal insulation chamber was installed to isolate the entire testing device from the environmental temperature.

Fig. 2 Assembled X-Y-Z stage to adjust the position of the punch on a specimen



Fig. 3 The assembled impression creep machine

A miniaturized cylindrical compression load-cell with a height of 45 mm and a diameter of 52 mm was used to monitor the impression force of the punch. It has a loading capacity of 20 N and is accurate to the mN scale. The cylindrical punch, with a diameter of 150 μm, was made of tungsten carbide. During the test, the impression depth was measured by a capacitive displacement gage which was accurate to 0.05μm. The load applied to the punch was measured by a load cell precise to the mN scale. The testing temperatures for the tests ranged from 323 to 623K in the chamber. The temperature was controlled to within ±0.1 K.

A CCD camera (magnification 150x) was used to align and monitor the contact of the punch to the tiny solder sample surface. The displacement and load signals were recorded using a data acquisition device (National Instrument, DAQ Card-6024). The data acquisition and control software used was ver. 8.0 LabVIEW, ver. 8.0. The finally assembled testing system is shown in Fig. 3.

### III. VALIDATION OF THE TESTING DEVICE

*3.1 Specimen preparation*

For the impression creep tests, pan-cake-shaped solder ball samples with a diameter of about 800 um were prepared after up-setting the solder ball with a diameter of 760 μm, as shown in Fig. 4. The chemical composition of the solder ally is shown in Table 1. The microstructure of the solder ball is shown in Fig. 5, showing a typical cast microstructure with dendrites. The primary dendrite arm spacing is approximately 6 μm.

After locating the specimen on the lower platen below the indenter, the assembly of specimen, indenter and platens was accommodated by the split furnace. The assembly was then heated to the test temperature and held there for at least 1 hour to establish thermal equilibrium in the testing arrangement before the specimen was impressed by the punch. Impression creep tests were performed in air using the developed impression creep machine. A type-K thermocouple was utilized to measure the temperatures at the specimen. The samples were tested at constant temperatures of 303K, 348K and 393K (0.8 $T_m$, $T_m$= 490 K) under constant stress levels. The impression stress levels ranged from 7 to 60 MPa.

TABLE I Chemical composition of the solder ball (wt.%)

| Element | Ag | Cu | Ge | Bi | Fe | Pb | Sb | Ni | Sn |
|---------|-----|-----|-----|-----|-----|-----|-----|-----|-----|
| wt.% | 2.9900 | 0.5260 | 0.0100 | 0.0009 | 0.0019 | 0.0241 | 0.0207 | 0.0032 | Rem |

*3.2 Preliminary creep tests for validation of the device*

Uniaxial creep behavior is often described by the well-known Sherby-Dorn equation,

$$\dot{\varepsilon} = A(\frac{DGb}{kT})(\frac{\sigma}{G})^n \quad (1)$$

where $\dot{\varepsilon}$ is the steady-state creep rate, A is the Dorn constant, D is the diffusion coefficient, b is the Burgers vector, k is Boltzmann's constant, G is the temperature-dependent shear modulus, σ is the applied stress, and T is the absolute temperature. An impression creep test yields the data of the impression velocity (*v*) versus the punch stress ($\sigma_p$), which is given by the following equation:

$$v = A_i(\frac{DGb}{kT})(\frac{\sigma_p}{G})^n \quad (2)$$

The equivalent uniaxial creep strain rate during impression creep may therefore be expressed as:

$$\dot{\varepsilon} = \beta \frac{v}{d} \qquad (3)$$

where d is a diameter of the indenter and β is a correlation factor with a typical value close to 0.755 [2]. Likewise, the punch stress $\sigma_p$ is proportional to the equivalent uniaxial stress σ, yielding,

$$\sigma = \frac{\sigma_p}{\alpha} \qquad (4)$$

where the correlation factors α has a typical value of 3.4 [2].



Fig. 4 Pan-cake-shaped solder ball with a diameter of about



Fig. 5 Optical micrographs of a solder ball sample

800 um after up-setting and a punch with a diameter of 150 um.

Calibration experiments of the displacement sensor and load sensor were carried out to evaluate and validate the performances of the developed device. Comparison tests based on the creep stress–strain rate curve were carried out with the custom-made testing device and considering previously reported data [6] on double-shear creep techniques for magnesium alloy (AZ31) to verify the feasibility of the testing device. Fig. 6 shows the steady-state creep rates by the self-made testing device and the data [6] for the double-shear creep techniques for magnesium alloy (AZ31). From Fig. 6, the creep data determined from the developed impression creep testing device show good correlations with those of the other creep testing techniques for AZ31. Thus, we verified the performance of the developed machine.

*3.3 Creep-rate curve*

The penetration depth of the indenter as a function of time at 303 K with $\sigma_p$ = 60 MPa is shown in Fig. 7. The figure shows a relatively long steady-state region with a short primary creep stage as the depth (h) increases linearly with time. The steady-state impression rate can then be determined by plotting d*h*/d*t* against time. As shown in this figure, the creep curve exhibits a very short primary creep state and thereafter the creep behavior enters a steady state. The curve then reaches a tertiary stage past a depth of 150 μm. According to this figure, the creep rate reaches a steady-state after 100 seconds, indicating that there is a very short primary creep state, compared to that in conventional uniaxial creep tests. Furthermore, an extensive secondary creep period occurs, compared to that in a uniaxial creep test. Past a depth of 230 μm, the strain rate is reduced dramatically, suggesting that the punch nearly penetrates the sample to a thickness of 550 μm and reaches the ceramic anvil. Therefore, the effective impression creep measuring range extends to nearly half of the sample thickness.
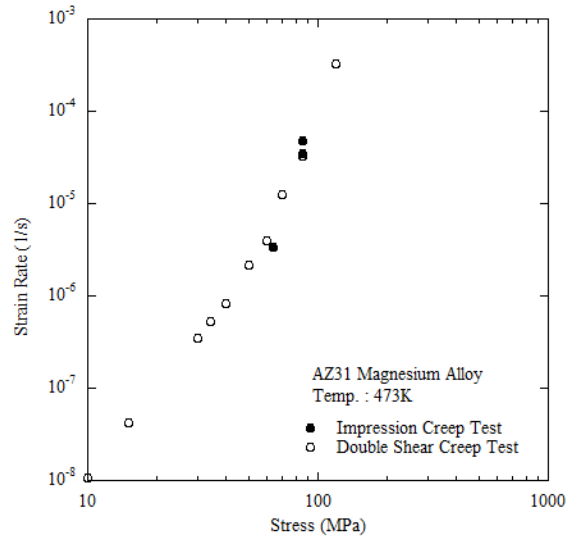
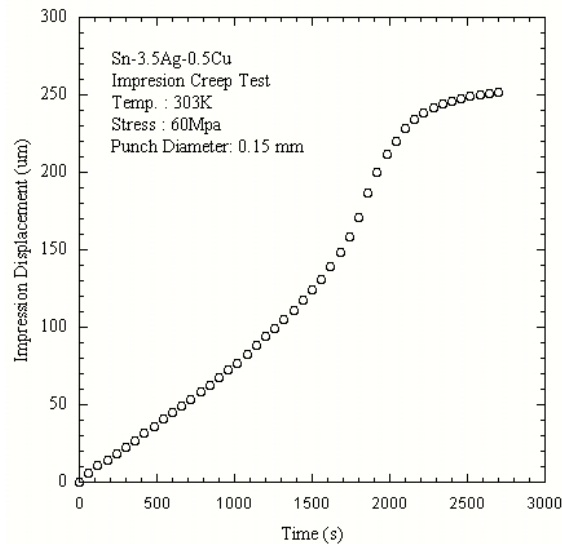Fig. 6 Comparison between data from impression creep tests and those from double-shear creep tests [6]



Fig. 7 Impression displacement and strain curve under 60 MPa at 303K

*3.4 Steady-state creep rates at various temperatures*

The samples were tested at constant temperatures ranging from 303K, 348K and 393K (0.8 $T_m$, $T_m$= 490 K) and under stresses ranging from 8 to 60 MPa. Fig. 8 shows a plot between the steady state creep rate and the stress. Fig. 8 shows that the value of the stress exponent, n (=$\partial$ln $\dot{\varepsilon}$ /$\partial$ln $\sigma_p$), is independent of the temperature and that there is significant variation in the stress exponent with the stress level. The value of the stress exponent was found to be 8.5 at the intermediate stress level at temperatures of 303K, 348K and 393K. The exponent of 8.5 indicates that the dominant creep deformation mechanism at the stress level is power-law break down [7]. However, the stress exponent changes from 8.5 to 12 at a higher stress level at 303K, indicating that there is another dominant creep deformation mechanism. The stress exponent change from 8.5 to 3.7 at approximately 20 MPa as the stress level decreases at 348K, indicating that the glide of dislocations dragging in a solute atmosphere is the dominant creep deformation mechanism [7]. At 393K, the same mechanism operates at stress levels that are lower than 20 MPa.

*3.5 Remarks on the developed testing device*

The conventional creep testing system cannot produce creep data at low creep rates and is limitateds in its ability to investigate actual solder joints less than 1 mm in diameter. Therefore, in this study, a micro-impression creep machine was designed and constructed in order to investigate the creep behavior of small solder balls within low creep-rate ranges. However, the developed machine frame was so sensitive to the environmental temperature that nanometer-scale displacement recording was unstable according to changes in the environmental temperature. We adopted a linear motion (LM) guide to prevent distortion of the punch rod. However, the tiny ball bearing in the LM guide cannot secure the smooth movement of the rod, resulting in

slightly jerky movement. Therefore, if these problems are solved, the testing machine can be expected to find use in evaluation of the creep strengths of microelectronic solder joints.
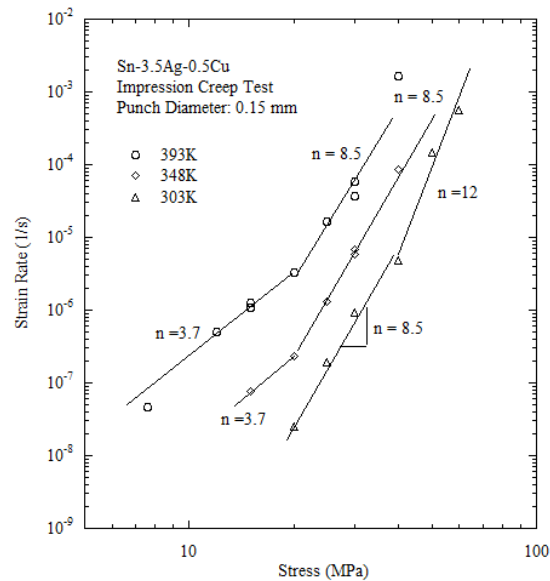


Fig. 8 Impression creep rate as a function of the stress at various temperatures.

## IV. CONCLUSION

In this study, a micro-impression creep machine was designed and constructed in order to investigate the creep behavior of small solder balls in low creep-rate ranges. The creep behavior of a lead-free solder ball (Sn-3.0Ag-0.5Cu) with a diameter of 760 μm was investigated. The samples were tested at constant temperatures of 303K, 348K and 393K (0.8 $T_m$, $T_m$= 490 K) and under stresses ranging from 8 to 60 MPa. We chose a dead weight system to ensure stable loading system which could function for a long time. A cylindrical punch with a diameter of 150 μm was used to investigate the creep behavior of the small solder ball with a diameter of less than 1 mm.

We verified the performance of the developed machine by comparing creep data from the self-made testing device with previously reported data for a magnesium alloy (AZ31). The effective impression creep measuring range was found to be nearly half of the sample thickness. The stress exponent for the solder ball sample was 3.7 at approximately 20 MPa at a temperature of 348K, indicating that the glide of dislocations dragging in a solute atmosphere was the dominant creep deformation mechanism. The testing machine performed adequately and is expected to be used to evaluate the creep strengths of microelectronic solder joints.

## ACKNOWLEDGMENT

## REFERENCES

[1]  I. Dutta, D. Pan, R.A. Marks, S.G. Jadhav, "Effect of thermo-mechanically induced microstructural coarsening on the evolution of creep response of SnAg-based microelectronic solders," Mat. Sci. Eng., A vol.410-411 , p.48-52, 2005.
[2]  J.C.M. Li, "Impression creep and other localized tests," Mat. Sci. Eng. A. vol.322 p.23-42, 2002.
[3]  F. Yang, L. Peng, "Impression creep of Sn3.5g eutectic alloy," Mat. Sci. Eng. A. Vol.409, pp.87-92, 2005.
[4]  R. Mahdudi, A.G. Geranmayeh, A. Rezaee-Bazzaze, "Impression creep behavior of lead-free Sn-5Sb solder alloy," Mat. Sci. Eng. A. Vol.448, pp.287-293, 2007.
[5]  D. Pan, R.A. Marks, R. Dutta, "Miniaturized impression creep testing of ball grid array solder balls attached to microelectronic packaging substrates, " Rev. Sci. Inst. Vol. 75, No.12, pp. 5244-5252, 2004.
[6]  K.T Yang, H.K. Kim, "Elevated temperature deformation behavior in an AZ31 magnesium alloy," J. Mech. Sci. Tech., vol. 20, no.8, p.1209-1216, 2006.
[7]  W.D. Nix and J.C. Gibering, "Mechanisms of time dependent flow and fracture of metals," Stanford University, 1993.